

# SELF-ACCELERATION OF A SPHERICALLY EXPANDING HYDROGEN-AIR FLAME AT ELEVATED PRESSURE

Kim, W.<sup>1</sup>, Sato, Y.<sup>1</sup>, Johzaki, T.<sup>1</sup>, Endo, T.<sup>1</sup>, Mogi, T.<sup>2</sup>, and Dobashi, R.<sup>2</sup>

<sup>1</sup> Department of Mechanical Systems Engineering, Hiroshima university, 1-4-1 Kagamiyama, Higashi-Hiroshima, 739-8527, Japan, kimwk@hiroshima-u.ac.jp

<sup>2</sup> Department of Chemical System Engineering, The University of Tokyo, 7-3-1 Hongo, Bunkyo-ku, Tokyo 113-8656, Japan

## ABSTRACT

Self-acceleration of a spherically expanding hydrogen-air flame was experimentally investigated in a closed dual-chamber apparatus with the quartz windows enabled to a flame diameter with up to 240 mm. The flame radius and flame speed in lean hydrogen-air mixtures at elevated pressure were evaluated using a high speed Schlieren photography. The experimental results from hydrogen-air explosion at elevated pressure validated the prediction model for self-similar propagation. The flame radius and its speed calculated by the prediction models agree well with the experimental results of hydrogen-air explosions at elevated pressure. Furthermore, the acceleration exponent  $\alpha$  is evaluated by plotting the flame radius with time. The results show the  $\alpha$  value increase with the dimensionless flame radius,  $r/r_{cl}$ . It is indicated that the self-acceleration and the transition regime to self-similar propagation exist in the spherically expanding hydrogen-air flame.

## 1.0 INTRODUCTION

In the accidental hydrogen-air explosions, the damage by a blast wave is strongly influenced by flame acceleration [1-6]. In the initial period, the self-acceleration of a spherically expanding hydrogen-air flame is occurred by Darrieus-Landau and diffusional-thermal instabilities. The onset of these instabilities are affected by the stretch, with the stabilizing influences of positive stretch. As the flame propagates, the flame speed increases due to the instabilities and it reach the self-similarity, and consequently the self-acceleration might lead to a detonation.

Gostinsev et al. [7] have suggested a semi-empirical formula for a self-similar propagation which derived from the experimental data of large atmospheric explosions. The self-similar propagation is given by:

$$r = r_0 + \frac{c_g \sigma^2 S_L^2 t^2}{\sqrt{\kappa}} \quad (1)$$

where  $r$  is the flame radius,  $r_o$  is the radius for the onset of self-acceleration,  $t$  is the time,  $\alpha$  is the acceleration exponent,  $c_g$  is a constant,  $\sigma = \rho_u/\rho_b$  is the volumetric expansion ratio,  $\rho_u$  is the density of unburned gas,  $\rho_b$  is the density of burned gas,  $S_L$  is the laminar burning velocity,  $\kappa$  is thermal diffusivity. Using Eq (1), the flame speed for the self-similar propagation can be rewritten as:

$$V_f = c_g \alpha \frac{(\sigma S_L)^{2\alpha-1}}{\kappa^{\alpha-1}} t^{\alpha-1} \quad (2)$$

These formula agree well with the large-scale explosions [1, 7, 8]. In addition, the value  $\alpha$  concluded  $\alpha=3/2$  for all mixtures in [7, 8], however, the various values of  $\alpha$  were reported in [2, 9-15]. However, we point out the inconvenience which the value of model constant  $c_g$  depends on the gas properties, although the authors proposed the value of model constant for all combustible gases is  $c_g = 2.0 \times 10^{-3}$  [16]. In the previous study, the model constant replaced the terms of gas properties and expressed as [16]:

$$c_g = (1-d)^{\frac{1}{1-d}} \left( \frac{\kappa}{r_c \sigma S_L} \right)^{\frac{d}{1-d}} \quad (3)$$

where  $d$  is the fractal excess defined as  $d = (\alpha-1)/\alpha$ ,  $r_{cl}$  is the critical flame radius for flame acceleration. Consequently, the prediction models for the flame speed as well as the blast wave is proposed using the fractal theory developed by Gostintsev et al [7]. These models were based on the fractal theory. The flame radius for self-similar propagation is given by [16]:

$$r = \left( \frac{1-d}{r_{cl}^d} \sigma S_L t + d r_{cl}^{1-d} \right)^{\frac{1}{1-d}} \quad (4)$$

The flame speed for self-similar propagation can be written as follows:

$$V_f = \frac{dr}{dt} = \sigma S_L \left( \frac{r}{r_{cl}} \right)^d \quad (5)$$

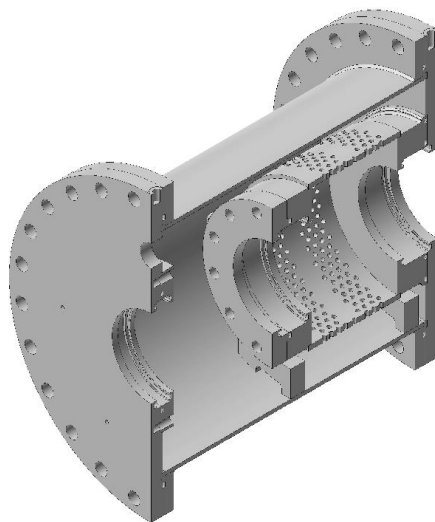
Details of formula derivation for self-similar propagation can be found in [16]. The predicted values are in agreement with those from the large atmospheric explosions. An important question is whether the prediction model can also cover hydrogen-air flame at an elevated pressure. An objective of the present paper is to validate the prediction model for self-similar propagation with

in the elevated pressure. Another objective is to investigate the self-similarity of hydrogen explosions in the elevated pressure with the results from large atmospheric hydrogen-air explosions.

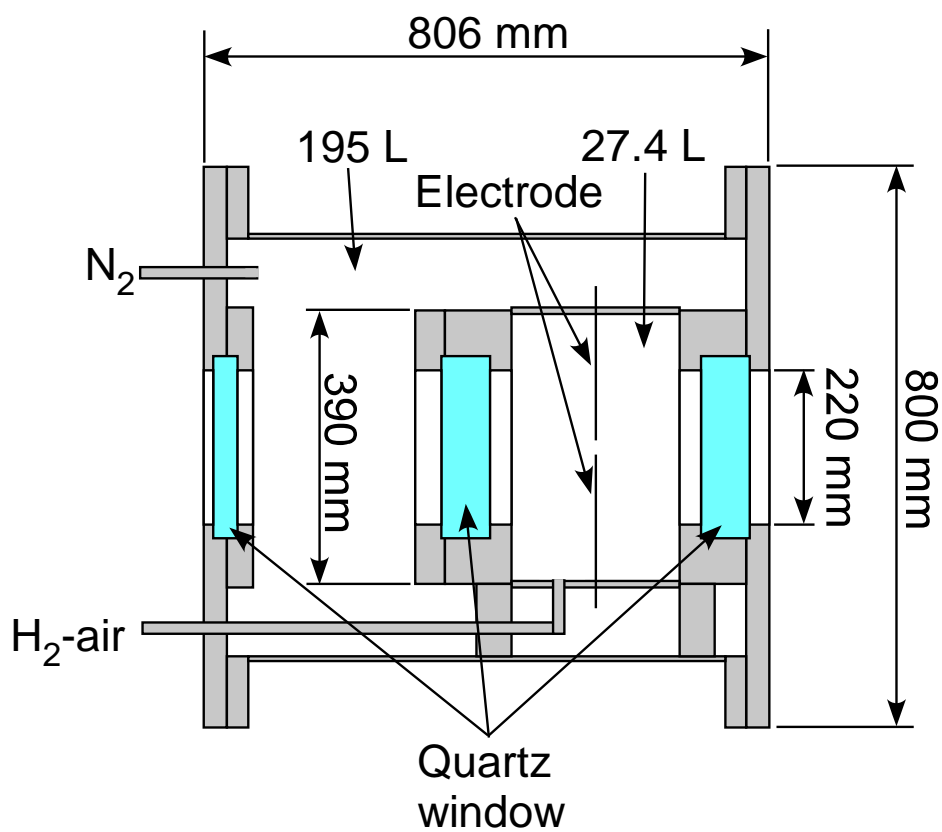
## 2.0 EXPERIMENTAL AND COMPUTATIONAL SPECIFICATIONS

In order to investigate the self-acceleration of a spherically expanding hydrogen-air flame, we have developed a dual-chamber apparatus enabled to observe a high-pressure spherical flame diameter with up to 240 mm. This apparatus referenced the high-pressure combustion apparatus developed in Princeton University [17] and extended the scale of the vessels. Figure 1 shows the three-dimensional and two-dimensional schematic drawings of the dual-chamber apparatus. It consists of two cylindrical chambers with three quartz windows. The size of two quartz windows is 260 mm diameter, 70 mm thickness and one is 260 mm diameter, 35 mm thickness). The volume of inner vessel is 27.4 L with 381.5 mm inner diameter, 406.9 mm outer diameter and 462 mm length including three flanges. The volume of outer vessel is 195.5 L with 590.6 mm inner diameter, 609.6 mm outer diameter and 860 mm length including two flanges. The holes with 10 mm diameter in the lateral walls of the inner vessel are pierced, as shown in Fig. 1 (a). In order to reduce the effect of increasing pressure in the vessel on the propagation behaviors, a thin polyethylene plastic film of 50  $\mu\text{m}$  thickness covered the lateral walls of the inner vessel and ripped by pressure increase.

The experiments were conducted in the dual-chamber apparatus. The hydrogen-air mixture initially filled in the inner, and nitrogen supplied to outer vessels at the same pressure. The hydrogen-air mixture at the center of the inner vessel is ignited by two electrodes of 50  $\mu\text{m}$  diameter. The behaviors of flame propagation were imaged with schlieren photography and recorded using a high-speed camera (Photron, FASTCAM Mini AX 50) at 5000 frames per second. In this study, the edge of flame front was detected by a canny edge method using MATLAB. The flame radius is defined as  $r = \sqrt{A/\pi}$ , where  $A$  is the flame area. Details of the image analysis are in [2]. In this study, the  $S_L$ , the  $\sigma$ , the laminar flame thickness,  $\delta = \lambda/\rho_u c_p S_L$ , where  $\lambda$  is the thermal conductivity of unburned gas,  $c_p$  is the thermal conductivity of unburned gas, were calculated by using Chemkin-Pro software [18] with the GRI Mech 3.0 reaction model [19].



(a) Three-dimensional schematic drawings.



(b) Two-dimensional schematic drawings.

Figure 1. Three-dimensional and two-dimensional schematic drawings of the dual-chamber apparatus.

### 3.0 RESULTS AND DISCUSSION

#### 3.1 Flame morphology

Figure 2 shows the images of outwardly propagating spherical flames for hydrogen-air mixture of  $\phi = 0.7$  at  $P_i = 0.07, 0.2$  MPa, whose Lewis number is less than unity ( $Le < 1$ ). The onset of long cracks observed in the initial stage of observation and the large cracks moved along the region of high curvature, and cells are created by the crack propagation across the existing cells. The cell divided spontaneously into smaller cells, and consequently the flame surface was covered fully by cell. The fully established cellular flame structure at  $P_i = 0.2$  MPa appeared earlier than that at  $P_i = 0.07$  MPa. This is because the flame thickness decrease with an increase in initial pressure, enhancing Darrieus-Landau and diffusional-thermal instabilities.

In this study, the critical flame radius for the fully developed cellular structure leads to the flame acceleration,  $r_{cl}$ , was evaluated by plotting between the measured flame speed and the stretch rate,  $K = (2/r)dr/dt$ , because the stretching in the initial period of propagations suppressed the development of the instability. The estimated value of  $r_{cl}$  at  $P_i = 0.2$  MPa is smaller than that at  $P_i = 0.07$  MPa due to Darrieus-Landau and diffusional-thermal instabilities.

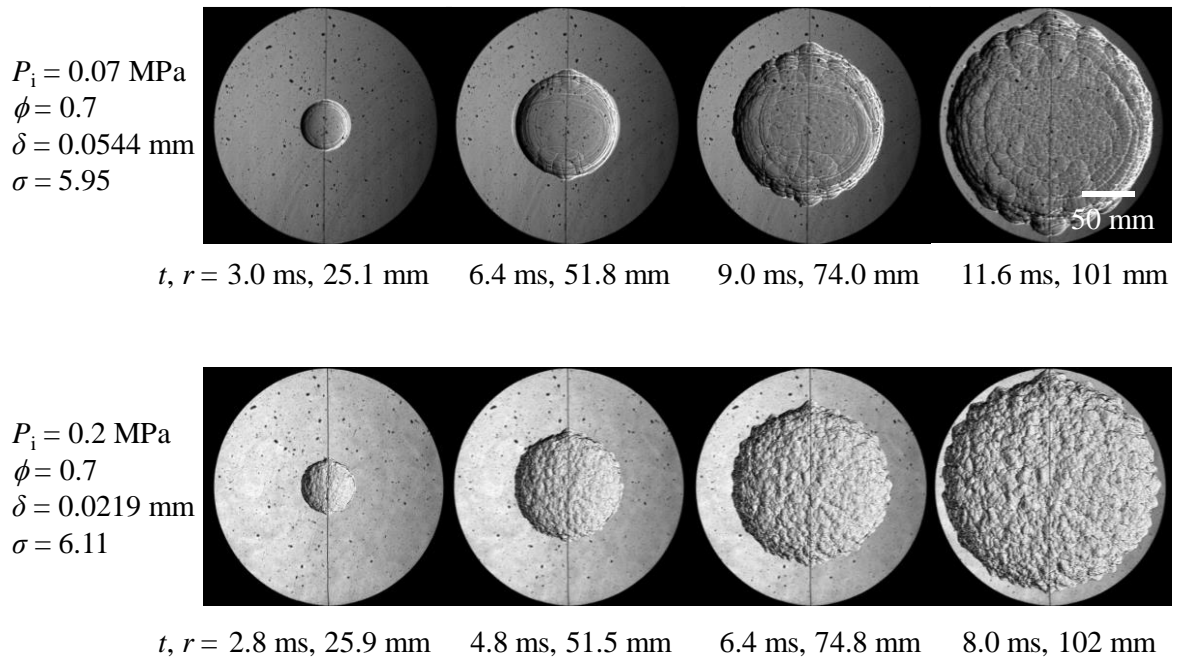


Figure 2. Schlieren images of hydrogen-air flames of  $\phi = 0.7$  at  $P_i = 0.07, 0.2$  MPa.

### 3.2 Self-acceleration

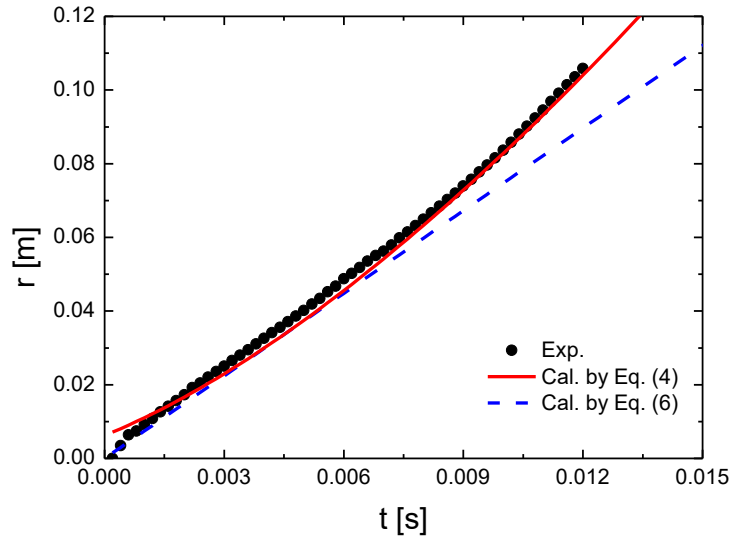
In order to investigate the self-acceleration, the measured flame radius and its speed compared with those for laminar and self-similar conditions. Under the assumptions that concentration of hydrogen-air mixture is uniform in quiescent flow fields, the instantaneous radius for the laminar spherical flame without the wrinkling on the flame surface can be written as:

$$r = \sigma S_L t \quad (6)$$

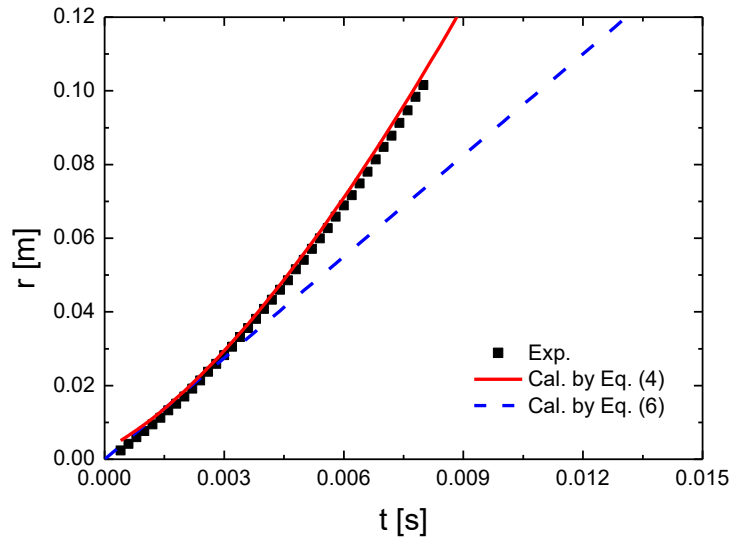
Then, the laminar flame speed can be rewritten as:

$$V_f = \frac{dr}{dt} = \sigma S_L \quad (7)$$

These models show that the speed for the laminar expanding spherical flame is constant. Figure 3 show the comparison between the flame radius in the experiment and those calculated by Eq. (4) and Eq. (6) for hydrogen-air flames of  $\phi = 0.7$  at  $P_i = 0.07, 0.2$  MPa. Dashed blue line in Fig. 3 represents the time history of flame radius evaluated by Eq. (4), implying the flame spherically expands without the wrinkling on the surface. During the initial period of the propagation, the flame radius calculated by Eq. (6) is in agreement with the experimental data. As the flame radius becomes larger, the measured radius is faster than that calculated by Eq. (6). It is demonstrated that the flame acceleration occurs in the experiments. Solid red curve represents the results estimated by Eq. (4). Eq. (4) based on the self-similar propagation agree well with experimental data in the acceleration regime.



(a)  $P_i = 0.07$  MPa

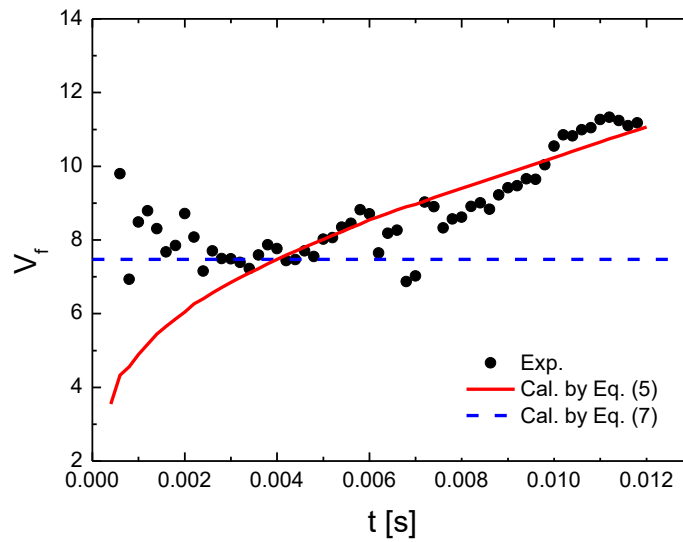


(b)  $P_i = 0.2$  MPa

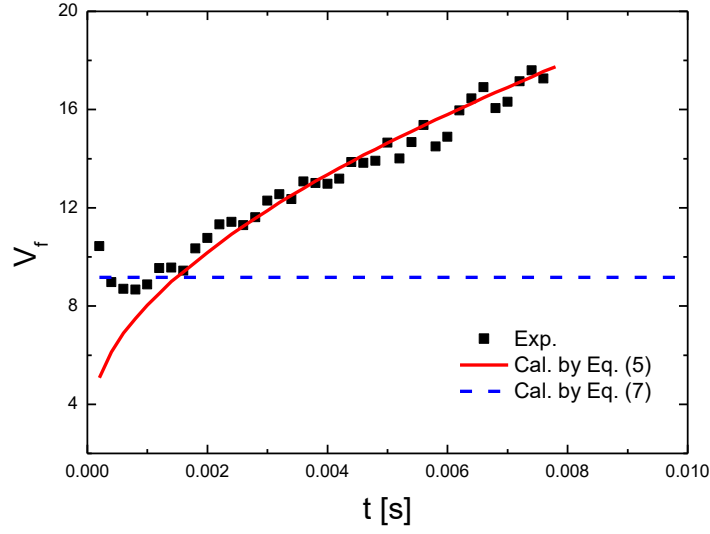
Figure 3. Comparison between measured flame radius of experiment and Eq. (4), Eq. (6) for hydrogen-air flames of  $\phi = 0.7$  at  $P_i = 0.07, 0.2$  MPa.

In Fig. 4, the measured flame speed is compared with the evaluated value by Eq. (5) and Eq. (7). Dashed blue line and solid red curve in Fig. 4 are the values calculated by Eq. (5) and Eq. (7), respectively. It was also found that the measured flame speed agrees initially with laminar flame

speed calculated by Eq. (7), thereafter it is much faster than that calculated by Eq. (7) as the size of flame becomes larger. The value calculated by Eq. (5) is in agreement with the experimental data in the acceleration stage of the propagation. The onset of flame acceleration at  $P_i = 0.2$  MPa is faster than that at  $P_i = 0.07$  MPa, because of a decrease in the flame thickness with an increase in initial pressure. This tendency of result also be in accord with the evaluation of the critical flame radius. Such results demonstrate that in the initial stage of the propagation the flame propagate smoothly, and its speed is close to laminar flame speed. As the flame becomes larger, at  $r > r_{cl}$ , the flame speed increases. It is confirmed that the speed can be estimated by the developed models by using fractal theory.



(a)  $P_i = 0.07$  MPa



(b)  $P_i = 0.2$  MPa

Figure 4. Comparison between measured flame speed and Eq. (5), Eq. (7) for hydrogen-air flames of  $\phi = 0.7$  at  $P_i = 0.07, 0.2$  MPa.

The acceleration exponent,  $\alpha$ , is estimated by plotting the flame radius versus time in the range between  $r_{cl}$  and 110 mm. Figure 5 shows the evaluated acceleration exponent as a function of  $\phi$ . The open square (0.07 MPa) and triangle (0.2 MPa) data points from a high-pressure apparatus (total volume  $V = 0.76$  L) enabled to measure the flame radii with up to 35 mm are also presented [16]. For hydrogen-air flames of  $\phi = 0.7$  at  $P_i = 0.2$  MPa, the value of the exponent,  $\alpha = 1.37$ , in the present experiment ( $V = 195.5$  L) is larger than  $\alpha = 1.26$  in the previous work ( $V = 0.79$  L), notwithstanding the same condition. It is indicated that the value of  $\alpha = 1.37$  further cover the self-acceleration regime than  $\alpha = 1.26$ . In other words, the values of the exponent are affected by the scale of flame.

Figure 6 shows the acceleration exponent as a function of  $r/r_{cl}$ . The open diamond data point in Fig. 6 is from the large-scale hydrogen-air explosions in a regular cubic plastic tent (total volume  $V = 27000$  L) covered a thin polyethylene sheet of 0.1 mm thickness [6]. Flame radii for hydrogen-air mixtures were observed up to about 1 m. The  $\alpha$  increased with increasing the  $r/r_{cl}$  and it saturated the value for self-turbulization suggested by Gonstinev et al. [7]. This trend is similar to those reported previously in [2, 6]. Such result indicated that the flame is stable at the small radii. As the flame propagates, flame speed increases due to the instabilities, and consequently

the accelerative dynamics reach the self-similar regime, i.e. the transition regime to self-turbulization exists during the flame propagation. However, further study on the relationship between  $\alpha$  and  $r/r_{cl}$  is necessary, because the data is insufficient to conclude the self-similar propagation.

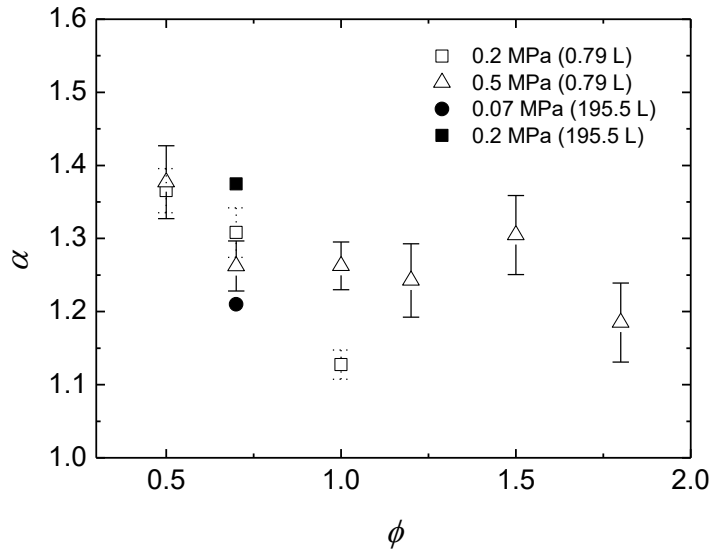


Figure 5. Acceleration exponents as a function of  $\phi$

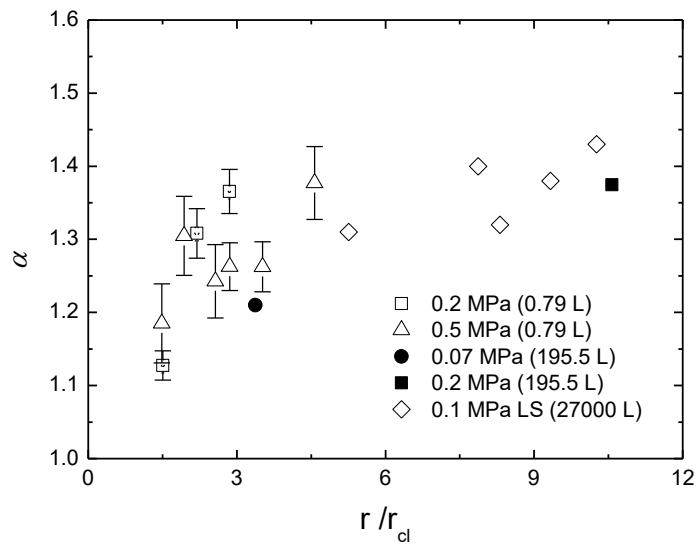


Figure 6. Acceleration exponents as a function of  $r/r_{cl}$ .

#### 4.0 CONCLUDING REMARKS

Self-acceleration of a spherically expanding hydrogen-air flame at elevated pressure was experimentally investigated using developed a dual-chamber apparatus. The experimental data from hydrogen-air explosion at elevated pressure validated the prediction model for self-similar propagation in agreement with large atmospheric hydrogen-air explosions. In the self-acceleration regime, the measured radius and its speed of hydrogen-air flame at elevated pressure agree well with those estimated by the prediction models developed by using the fractal theory. It is indicated that the model based on the concept of self-similarity is not merely predictable data in large atmospheric hydrogen-air explosions but also those hydrogen-air explosions at elevated pressure. In addition, the value of  $\alpha$  is evaluated. The  $\alpha$  values increased with an increase in  $r/r_{cl}$ , implying the transition regime from the stable regime to self-similar regimes exists in the flame propagation.

#### ACKNOWLEDGEMENTS

This study was supported by JSPS KAKENHI Grant Numbers 18H03822, 18K13958.

#### REFERENCES

- [1] Dobashi, R., Kawamura, S., Kuwana, K., and Nakayama, Y., Consequence analysis of blast wave from accidental gas explosions, *Proceedings of the Combustion Institute*, **33**, 2011, pp. 2295-2301.
- [2] Kim, W., Sato, Y., Johzaki, T., Endo, T., Shimokuri, D., and Miyoshi, A., Experimental study on self-acceleration in expanding spherical hydrogen-air flames, *International Journal of Hydrogen Energy*, **43**, 2018, pp.12556-12564.
- [3] Kim, W.K., Mogi, T., and Dobashi, R., Flame acceleration in unconfined hydrogen/air deflagrations using infrared photography, *Journal of Loss Prevention in the Process Industries*, **26**, 2013, pp.1501-1505.
- [4] Kim, W.K., Mogi, T., and Dobashi, R., Fundamental study on accidental explosion behavior of hydrogen-air mixtures in an open space, *International Journal of Hydrogen Energy*, **38**, 2013, pp. 8024-8029.
- [5] Kim, W.K., Mogi, T., Dobashi, R., Effect of propagation behaviour of expanding spherical flames on the blast wave generated during unconfined gas explosions, *Fuel*, **128**, 2014, pp. 396-403.
- [6] Kim, W.K., Mogi, T., Kuwana, K., and Dobashi, R., Self-similar propagation of expanding spherical flames in large scale gas explosions, *Proceedings of the Combustion Institute*, **35**, 2015, pp. 2051-2058.

- [7] Gostintsev, Y.A., Istratov, A.G., and Shulenin, Y.V., Self-Similar Propagation of a Free Turbulent Flame in Mixed Gas-Mixtures, *Combust Explosions and Shock Waves*, **24**, 1988, pp. 563-569.
- [8] Bradley, D., Instabilities and flame speeds in large-scale premixed gaseous explosions, *Philosophical Transactions of the Royal Society A: Mathematical, physical and engineering sciences*, **357**, 1999, pp. 3567-3581.
- [9] Bauwens, C.R., Bergthorson, JM., and Dorofeev, SB., Experimental study of spherical-flame acceleration mechanisms in large-scale propane-air flames, *Proceedings of the Combustion Institute*, **35**, 2015, pp. 2059-2066.
- [10] Bauwens, C.R., Bergthorson, JM., and Dorofeev, SB., Experimental investigation of spherical-flame acceleration in lean hydrogen-air mixtures, *International Journal of Hydrogen Energy*, **42**, 2017, pp. 7691-7697.
- [11] Gostintsev, Y.A., Fortov, V.E., and Shatskikh, Y.V., Self-similar propagation law and fractal structure of the surface of a free expanding turbulent spherical flame, *Doklady Physical Chemistry*, **397**, 2004, pp. 141-144.
- [12] Karlin, V., and Sivashinsky, G., The rate of expansion of spherical flames, *Combustion Theory and Modelling*, **10**, 2006, pp. 625-637.
- [13] Liberman, M.A., Ivanov, M.F., Peil, O.E., Valiev, D.M., and Eriksson, L.E., Self-acceleration and fractal structure of outward freely propagating flames, *Physics of Fluids*, **16**, 2004, pp. 2476-2482.
- [14] Wada, Y., and Kuwana, K., A numerical method to predict flame fractal dimension during gas explosion, *Journal of Loss Prevention in the Process Industries*, **26**, 2013, pp. 392-395.
- [15] Wu, F., Jomaas, G., and Law, C.K., An experimental investigation on self-acceleration of cellular spherical flames, *Proceedings of the Combustion Institute*, **34**, 2013, pp. 937-945.
- [16] Kim, W.K., Mogi, T., Kuwana, K., and Dobashi, R., Prediction model for self-similar propagation and blast wave generation of premixed flames, *International Journal of Hydrogen Energy*, **40**, 2015, pp. 11087-11092.
- [17] Tse, S.D., Zhu, D.L., and Law, C.K., Optically accessible high-pressure combustion apparatus, *Review of Scientific Instruments*, **75**, 2004, pp. 233-239.
- [18] <http://www.ansys.com/products/fluids/ansys-chemkin-pro>.
- [19] <http://combustion.berkeley.edu/gri-mech/>.